Trajectory and Dispersion of Vapor and Drop Clouds in Evaporating Diesel Spray Injected into Model Combustion Chamber

M.Suzuki*, K.Nishida and H.Hiroyasu
Department of Mechanical Engineering
University of Hiroshima
1-1-1 Kagamiyama, Higashi-Hiroshima 724
Japan
* *Idemitsu Kosan Co., Ltd.*

ABSTRACT

A new laser based method for simultaneous imaging of drops and vapor in an evaporating fuel spray was applied to a Diesel spray injected into a two-dimensional model combustion chamber of a direct injection (D.I.) Diesel engine settled in a high-pressure and high-temperature vessel. The imaging method was based on extinction of two-wavelength, that is, ultraviolet (λ=280 nm) and visible (λ=560 nm) laser lights through the fuel spray due to absorption by the vapor and scattering by the drops. The results of the imaging supply two-dimensional distributions of the line-of-sight transmissivities along the optical path in the drops and the vapor in the fuel spray. Clarification was made of effects of several combustion system variables, such as injection pressure, piston cavity radius, injection angle, nozzle projection and top clearance, on the distributions of the drops and the vapor in the D.I. Diesel combustion chamber.

INTRODUCTION

A recently developed fuel injection system with high injection pressure for a direct injection (D.I.) Diesel engine has a potential for an advanced combustion system to achieve fairly low exhaust emissions and superior fuel economy. Lots of studies have been made to clarify roles of the fuel spray with high injection pressure and other combustion system variables, such as combustion chamber shapes and air flow characteristics, in controlling mixture formation and subsequent combustion in the D.I. Diesel engines (1-3). However, detailed explanation mentioned above could not be made for lack of qualitative or quantitative information of the phenomena proceeding in the combustion chamber. Especially, information of trajectory and dispersion of the fuel spray, which consists of drops and vapor, injected into the combustion chamber is essential to the development of the advanced combustion system for further reducing exhaust emissions as well as improving fuel economy.

In this study, a new laser-based method using α-methylnaphthalene as the injection fuel (4-6) was applied to the simultaneous and qualitative imaging of drops and vapor in the evaporating Diesel spray injected into a two-dimensional model combustion chamber settled in a high-temperature and high-pressure vessel. The imaging method was based on extinction of two-wavelength, that is, ultraviolet (λ=280 nm) and visible (λ=560 nm) laser lights through the fuel spray due to absorption by the vapor and scattering by the drops. Subtraction of the transmissivity of the visible laser light from that of the ultraviolet laser light made it possible to image the distribution of the vapor in the fuel spray. The distribution of the drops is imaged by the transmissivity of the visible laser light. The results of the imaging supply two-dimensional distributions of the line-of-sight transmissivities along the optical path in the drops and the vapor in the fuel spray.

Several combustion system variables of the D.I. Diesel engine were changed such as injection pressure, piston cavity diameter, injection angle, nozzle projection length and top clearance. Effects of these variables on the distributions of the vapor and the drops in the model combustion chamber were made clear.

EXPERIMENTAL APPARATUS AND PROCEDURE

Measuring System

Figure 1 shows a schematic diagram of optical arrangement. Ultraviolet laser light (λ=280 nm) and visible laser light (λ=560 nm) from a DYE laser (Lambda Physic:LPD3002) induced by a Nd:YAG laser (Continuum:NY-61-10, 300mJ/6ns at 532nm) were separated into two-wavelength laser lights through a dichroic mirror. Each laser beam was filtered by an attenuator for adjusting the intensity and was collimated to the parallel laser light of 100 mm in diameter. Then, two wavelength parallel laser lights were composed and passed through the Diesel spray injected into the model combustion chamber settled in a high pressure and high temperature vessel.

α-methylnaphthalene ($C_{10}H_7(CH_3)$) was selected as an injection fuel, since it absorbs the ultraviolet laser light but does not absorb the visible laser light. Table 1 shows the comparison of the fuel properties between α-methylnaphthalene and Diesel fuel No.2. There is a comparative good agreement between their properties.

The transmitted laser lights absorbed and scattered by the

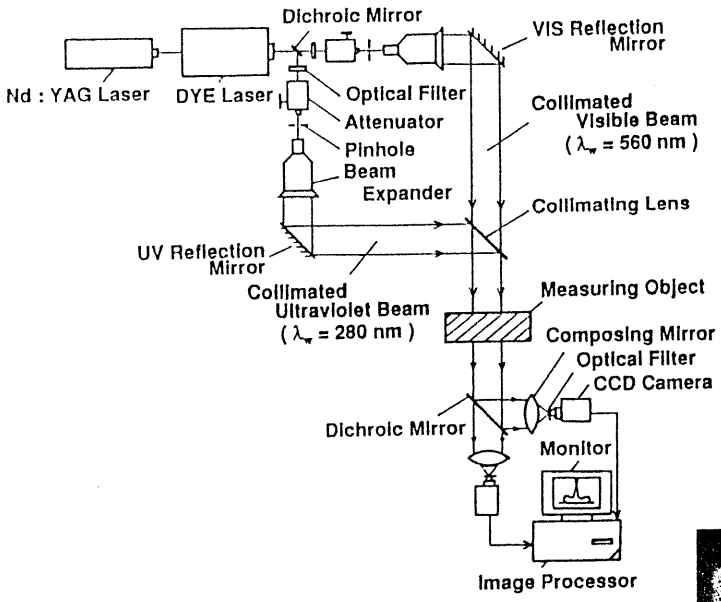

Fig.1 Measuring system

Table 1 Properties of α-methylnaphthalene

	α - Methylnaphthalene $C_{10}H_7(CH_3)$	Diesel Fuel JIS No.2
Molecular Weight	142.2	180 (mean)
Density kg/m³	1.0163 x 10³	0.8309 x 10³
Kinematic Viscosity m²/s	2.575 x 10⁻⁶ (at 30 ℃)	3.822 x 10⁻⁶
	1.761 x 10⁻⁶ (at 50 ℃)	2.547 x 10⁻⁶
	1.300 x 10⁻⁶ (at 70 ℃)	1.840 x 10⁻⁶
Surface Tension N/m	38.6 x 10⁻³	28.2 x 10⁻³
Boiling Point K	517.8	546.0
Critical Temperature K	772.0	———
Critical Pressure MPa	3.45	———

vapor and the drops in the fuel spray were separated into two-wavelength laser lights and captured with two CCD camera systems (Photometrics:Star1, 384 x 576 pixels, 23μm x 23μm/pixel), respectively. Resulting images were digitized in a computer and calculation was made of distributions of the transmissivities due to the vapor and the drops in the Diesel spray.

Model Combustion Chamber and Injection System

Figure 2 shows a schematic drawing of the model combustion chamber and definition of symbols such as the cylinder radius $D_c/2$, the piston cavity radius $d_c/2$, the top clearance δ, the nozzle projection length L_n, and the injection angle α.

An injection system was for a D.I. Diesel engine. Fuel was injected from a single hole nozzle. A single fuel injection was made by controlling the rack of an in-line-type injection pump with an electric actuator.

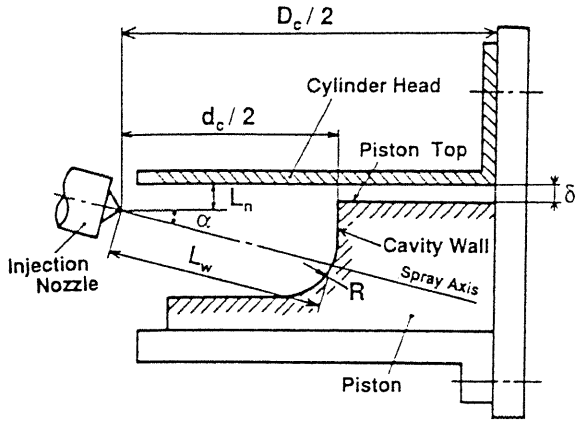

Fig.2 Model combustion chamber

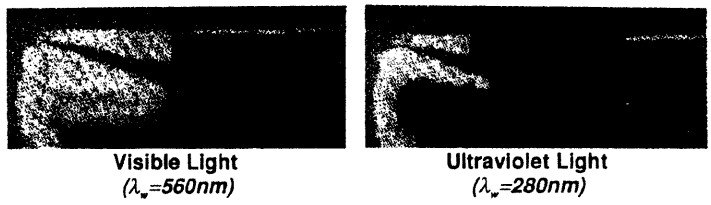

(a) Original images

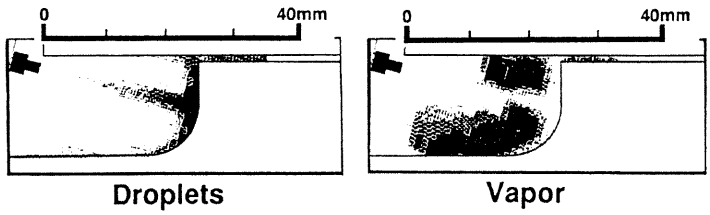

(b) Results of imaging

Fig.3 Processing of images

Principle for Imaging Vapor and Drops

Figures 3 (a) and (b) show original images of the evaporating Diesel spray illuminated by visible and ultraviolet laser lights, and the results of imaging of the drops and the vapor in the Diesel spray. The visible laser light (λ=560nm), which is not absorbed by both liquid and vapor phases, is attenuated only by scattering by the drops. So the transmissivity of the visible laser light by the Diesel spray is equal to the transmissivity due to only scattering by the liquid drops $\log(I_0/I_t)_{Lsca}$.

The ultraviolet laser light (λ=280nm), which is absorbed by both liquid and vapor phases, is attenuated due to scattering by the drops, absorption by the drops and the vapor. At a region where the transmissivity of laser light is less than 1.1, that is, the transmitted light intensity is more than 8% of the incident light intensity, the absorption of the ultraviolet laser light by the drops in the spray was negligible (3-5). So the transmissivity of the ultraviolet laser light by the Diesel spray is expressed by the summation of the transmissivity due to scattering by the liquid drops $\log(I_0/I_t)_{Lsca}$ and absorption by the vapor $\log(I_0/I_t)_{Vabs}$. From the measured result using the visible laser light, the transmissivity only due to

scattering by the drops, $\log(I_0/I_t)_{Lsca}$, can be expressed as Eq.(1). And from the difference in the transmissivity between the ultraviolet and visible laser lights, the transmissivity only due to absorption by the vapor, $\log(I_0/I_t)_{Vabs}$, can be expressed as Eq.(2).

$$\log\left(\frac{I_0}{I_t}\right)_{Lsca} = \log\left(\frac{I_0}{I_t}\right)_{\lambda=560nm} \quad (1)$$

$$\log\left(\frac{I_0}{I_t}\right)_{Vabs} = \log\left(\frac{I_0}{I_t}\right)_{\lambda=280nm} - \log\left(\frac{I_0}{I_t}\right)_{\lambda=560nm} \quad (2)$$

Experimental Conditions

Table 2 shows experimental conditions. Nitrogen was used as ambient gas. Standard ambient temperature and pressure were T_a=773 K and P_a=2.9 MPa, respectively, which simulated the ambient air condition in the combustion chamber of a D.I. Diesel engine at the top dead center. Ambient temperature was changed from T_a=773 K to 573 K and 293 K under the constant ambient gas density of ρ_a=12.5 kg/m^3. An injection nozzle had a single hole with a diameter of d=0.15 mm and a length-to-diameter ratio of l/d=8.7. The valve opening pressure and the amount of fuel injected were set to P_0=19.6 MPa and m_f=20.4 mg, respectively. A cylinder radius was fixed at D_c/2=67.5 mm.

Effective injection pressure ΔP_i, a cavity radius d_c/2, an injection angle α, a nozzle projection length L_n and a top clearance δ were changed as shown in the table. The effective injection pressure ΔP_i was defined as differential pressure between injection line pressure averaged during the injection period and ambient gas pressure. The standard experimental condition was ΔP_i=85 MPa for the effective injection pressure, and for the dimensions of the model combustion chamber, d_c/2=25 mm, α=15 deg., L_n=1 mm and δ=1 mm.

Table 2 Experimental conditions

Ambient Gas		Nitrogen
Ambient Temperature	T_a	773, 573, 293 K
Ambient Pressure	P_a	2.9, 2.2, 1.1 MPa
Ambient Density	ρ_a	12.5 kg/m^3
Injection Nozzle		Hole Nozzle
Number of Hole		1
Nozzle Diameter	d	0.15 mm
l/d		8.7
Valve Opening Press.	P_0	19.6 MPa
Effective Injection Press.	ΔP_i	56, 68, 85 MPa
Cylinder Diameter	D_c/2	67.5 mm
Cavity Diameter	d_c/2	15, 25, 35 mm
Impingement Angle	α	10, 15, 20 deg.
Nozzle Projection	L_n	1, 6 mm
Top Clearance	δ	1, 4 mm

RESULTS AND DISCUSSIONS

Temporal Development of Spray

Figure 4 shows temporal developments of the drops and

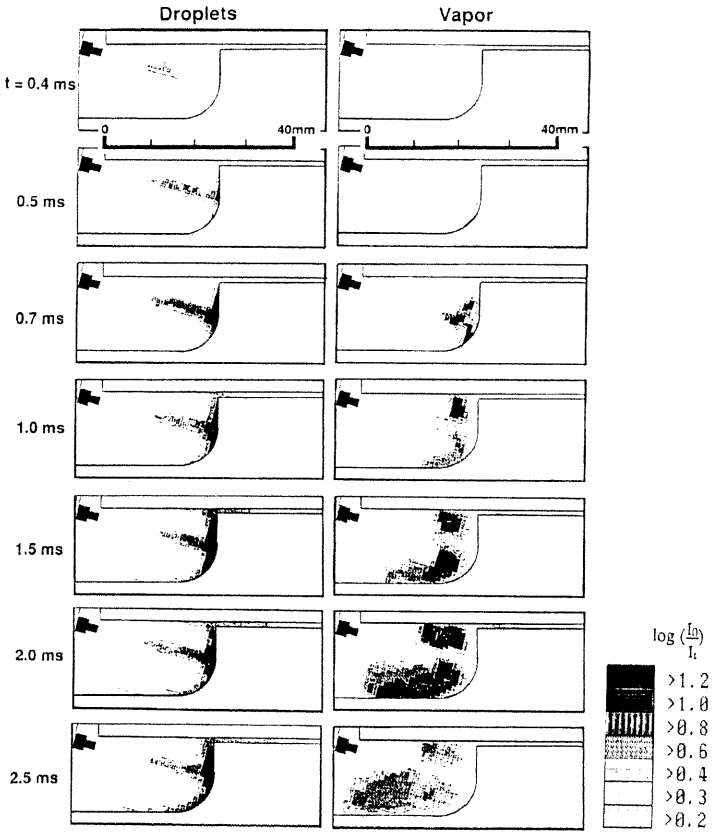

Fig.4 Temporal development of drops and vapor in model combustion chamber
(ΔP_i=85 MPa, d_c/2=25 mm, α=15 deg., L_n=1 mm, δ=1 mm)

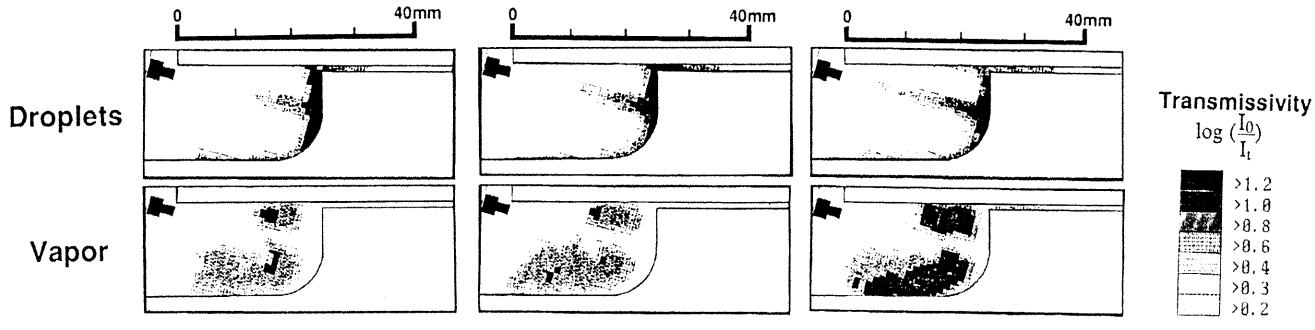

(a) ΔP_i=56 MPa (b) ΔP_i=68 MPa (c) ΔP_i=85 MPa

Fig.5 Effect of injection pressure
(d_c/2=25 mm, α=15 deg., L_n=1 mm, δ=1 mm, t=2.0 ms)

the vapor in the model combustion chamber under effective injection pressures of ΔP_i=85 MPa. The model combustion chamber has the standard dimensions.

The drops impinge on the cavity wall at t=0.5 ms after the start of injection, and the vapor appears around the impingement point of the drop on the cavity wall at t=0.7 ms. Then the drops develop toward the cavity bottom and the cylinder head along the cavity wall. The drops are distributed just in the vicinity of the walls of the cavity and the cylinder head. The vapor is not found in the vicinity of the cavity wall and at the impingement point of the drops. The vapor is distributed much wider than the drops in the space of the model combustion chamber, especially in the space of the cavity bottom side. The distribution of the vapor looks like enveloping the distributions of the drops along the walls of the model combustion chamber.

Effect of Injection Pressure

Figure 5 shows an effect of effective injection pressure ΔP_i on distributions of the drops and vapor at t=2.0 ms after the start of injection. As effective injection pressure is increased from ΔP_i=56 MPa to 85 MPa, the transmissivity and the area of the drops along the cavity wall is decreased, whereas the vapor with higher transmissivity is distributed wider in the space of the cavity. In the top clearance space, the drops with high transmissivity are distributed and the vapor is hardly seen under ΔP_i=56 MPa and 68 MPa. Increasing effective injection pressure to ΔP_i=85 MPa decreases the transmissivity of the drops and generates the vapor in the top clearance space.

Effect of Cavity Radius

Figure 6 shows distributions of the drops and the vapor for cavity radii of $d_c/2$=15 mm, 25 mm and 35 mm at t=2.0 ms after the start of injection. In the case of $d_c/2$=15 mm, the spray impinges on the cavity wall near the piston top. The drops are distributed along the cavity wall and penetrate into the top clearance space. The vapor is mainly distributed in the space of the cavity bottom side and is not seen in the top clearance space. In the case of $d_c/2$=35 mm, the spray impinges on the corner of the cavity bottom. The distribution of the drops on the cavity wall is at the narrow area around the impingement point. The vapor is distributed symmetrically around the drops and is not seen in the top clearance space. The widest distribution of the vapor with the highest transmissivity is found in the case of $d_c/2$=25 mm. The drops penetrate into the top clearance space and the vapor is seen in this space.

Effect of Injection Angle

Figure 7 shows an effect of an injection angle α on the distributions of the drops and the vapor at t=2.0 ms after the start of injection. The injection angle was varied from α=10 deg. to 20 deg. In the case of α=10 deg., the spray impinges

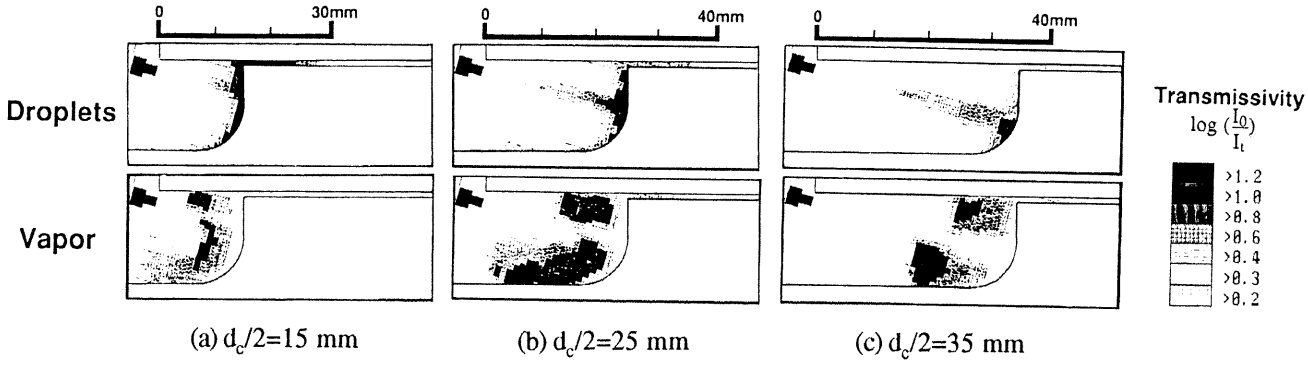

(a) $d_c/2$=15 mm (b) $d_c/2$=25 mm (c) $d_c/2$=35 mm

Fig.6 Effect of cavity radius
(ΔP_i=85 MPa, α=15 deg., L_n=1 mm, δ=1 mm, t=2.0 ms)

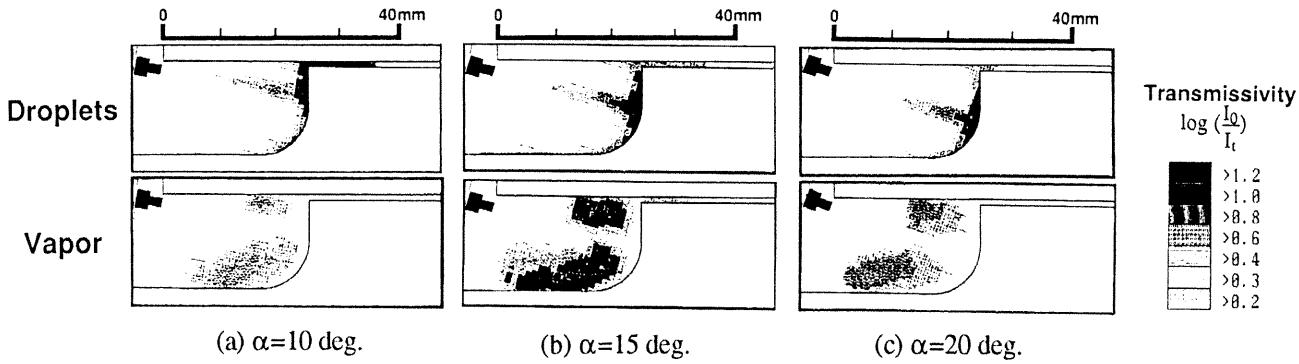

(a) α=10 deg. (b) α=15 deg. (c) α=20 deg.

Fig.7 Effect of injection angle
(ΔP_i=85 MPa, $d_c/2$=25 mm, L_n=1 mm, δ=1 mm, t=2.0 ms)

on the cavity wall near the piston top. The drops penetrate into the top clearance space but the vapor is not found in this space. Though a large amount of the drops must be in the cavity space of the cylinder head side, the distribution of the vapor in this space is not wide as compared with other injection angles, and the main distribution of the vapor is in the cavity space of the bottom side. In the case of α=20 deg., the spray impinges on the corner of the cavity bottom. Penetration of the drops into the top clearance space is weak and only a small amount of the vapor is seen in the top clearance space. An injection angle of α=15 deg. shows the widest distribution of the vapor with the highest transmissivity in the combustion chamber. Some drops penetrate into the top clearance space and the vapor is generated in this space.

The above results varying the cavity radius and the injection angle lead to a conclusion that the evaporation of the fuel drops and the dispersion of the vapor are enhanced under certain cavity radius and injection angle.

Effect of Nozzle Projection Length and Top Clearance

Figure 8 shows effects of a nozzle projection length L_n and a top clearance δ. An effect of injection timing on the distribution of the drops and the vapor can also be deduced from the results varying the top clearance.

The distributions of the drops and the vapor under the standard experimental condition, that is, L_n=1 mm and δ=1 mm, are shown in Fig. 8 (a). When the top clearance is increased to δ=4 mm as shown in Fig. 8 (b), the spray impinges on the cavity wall near the piston top. The distribution of the drops along the cavity wall is decreased, whereas the vapor with lower transmissivity is distributed wider in the combustion chamber than under the standard condition of δ=1 mm. The drops do not penetrate into the top clearance space and the vapor is seen in this space.

When the nozzle projection length is increased to L_n=6 mm under the top clearance is fixed to δ=1 mm as shown in Fig. 8 (c), the spray impinges on the bottom of the cavity. Most of the drops penetrate to the cylinder head side and into the top clearance space. Most vapor with high transmissivity is distributed in the relatively narrow space in the cavity of the cylinder head side. The vapor is not found in the top clearance space.

Increasing the top clearance space to δ=4 mm, as shown in Fig. 8 (d), resulst in a wider distribution of the vapor in the cavity space of both cylinder head side and cavity bottom side. In the top clearance space, the drops do not penetrate and the vapor is seen.

The above results lead to the conclusions that the moderate spray penetration along the cavity wall toward the cavity bottom side enhances the distribution of the vapor in the cavity space, and that increasing the top clearance reduces

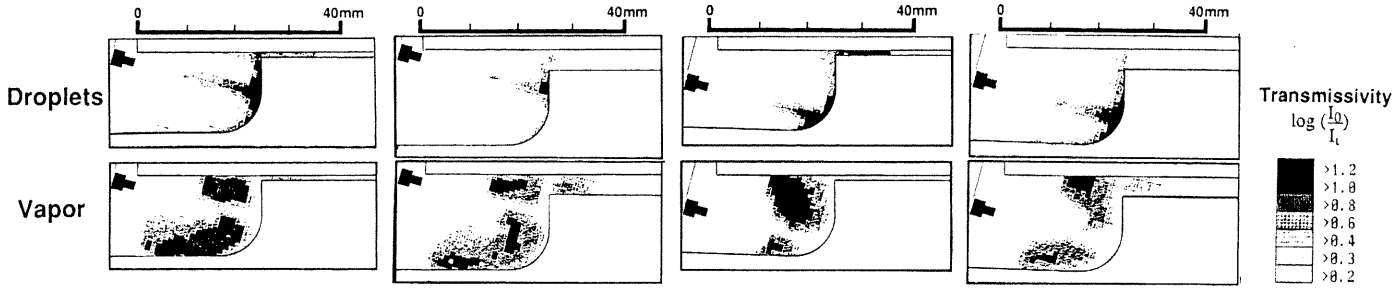

(a) L_n=1 mm, δ=1 mm (b) L_n=1 mm, δ=4 mm (c) L_n=6 mm, δ=1 mm (d) L_n=6 mm, δ=4 mm

Fig.8 Effects of nozzle projection length and top clearance
(ΔP_i=85 MPa, $d_c/2$=25 mm, α=15 deg., t=2.0 ms)

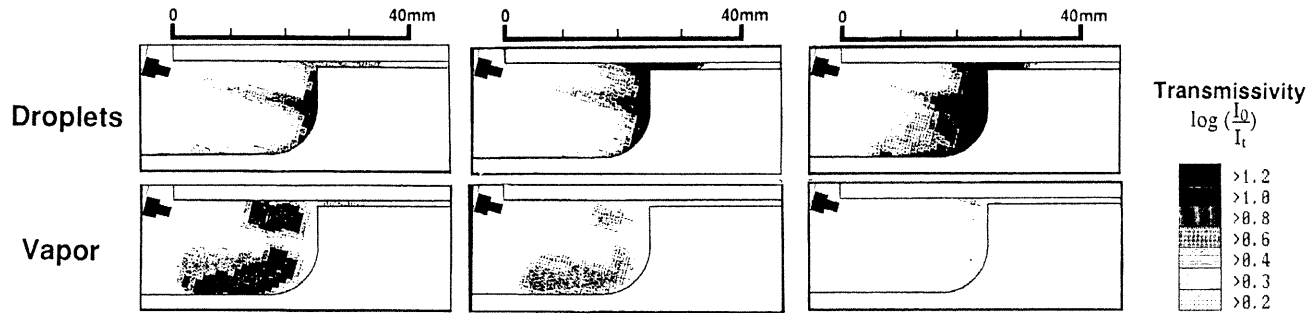

(a) T_a=773 K (b) T_a=573 K (c) T_a=293 K

Fig.9 Effect of ambient gas temperature
(ΔP_i=85 MPa, $d_c/2$=25 mm, α=15 deg., L_n=1 mm, δ=1 mm, t=2.0 ms)

the penetration of the drops into the top clearance space and enhances the generation of the vapor in this space.

Effect of Ambient Gas Temperature

Figure 9 shows an effect of ambient gas temperature T_a on the distributions of the drops and the vapor at t=2.0 ms after the start of injection. The vapor is faintly seen around the cavity wall near the piston top at ambient gas temperature of T_a=293 K, whereas the drops are found along the cavity wall. As the ambient gas temperature is increased, the distribution and the transmissivity of the vapor are increased in the space of the model combustion chamber. Increasing the ambient gas temperature enhances the evaporation of the fuel drops first at the cavity bottom side and next at the cylinder head side. The shape of the fuel distribution including the drops and the vapor is much different between T_a=773 K and 293 K, especially around the tip of the fuel spray along the cavity wall. This seems to be due to the expansion of fuel volume in the spray during the evaporation.

CONCLUSIONS

A new laser based method for simultaneous imaging of drops and vapor was applied to an evaporating Diesel spray injected into a two-dimensional model combustion chamber of a direct injection (D.I.) Diesel engine settled in a high-pressure and high-temperature vessel. Clarification was made of effects of several combustion system variables, such as injection pressure, piston cavity radius, injection angle, nozzle projection and top clearance, on the distributions of the drops and the vapor in the model combustion chamber. Main conclusions are summarized as follows:

(1) Drops are distributed just in the vicinity of the walls of the cavity and the cylinder head of the combustion chamber. Vapor is not found in the vicinity of the cavity wall and around the impingement point of the drops on the cavity wall. The vapor is distributed much wider than the drops in the space of the combustion chamber.

(2) As effective injection pressure is increased, the transmissivity and the area of the drops along the cavity wall is decreased, whereas the vapor with higher transmissivity is distributed wider in the space of the cavity. The transmissivity of the drops in the top clearance space is decreased and the vapor is generated in this space.

(3) The evaporation of the fuel drops and the dispersion of the vapor are enhanced under certain cavity radius and injection angle.

(4) Moderate spray penetration along the cavity wall toward the cavity bottom side enhances the distribution of the vapor in the cavity space. An increase in the top clearance reduces the penetration of the drops into the top clearance space and enhances the generation of the vapor in this space.

(5) As ambient gas temperature is increased, the distribution and the transmissivity of the vapor are increased in the space of the combustion chamber. Increasing the ambient gas temperature enhances the evaporation of the fuel drops first at the cavity bottom side and next at the cylinder head side.

(6) The shape of the fuel distribution including the drops and the vapor is much different between T_a=773 K and 293 K, especially around the tip of the fuel spray along the cavity wall.

ACKNOWLEDGMENT

This study was supported by ZEXEL Corp. and New A.C.E . Institute Co., Ltd. for providing injection equipments. The authors also wish to express their thanks to Mr. Katsuyuki Okamine, Mr. Hiroo Kotorida, Mr. Osamu Yamamoto and Mr. Kazutaka Shimada for their effort during the experiment.

REFERENCES

1. Hiroyasu, H, Nishida, K., Yoshikawa, S., Kwon, S. and Arai, M., "Combustion Process in a D.I. Diesel Engine with High-Pressure Injection - Effect of Spatial Distribution of Fuel Spray in a Combustion Chamber on NOx Emission -," Transactions of the Society of Automotive Engineers of Japan, Vol.22, No.4, pp.53-58, 1991. (in Japanese)
2. Ikegami, M., Fukuda, M., Yoshihara, Y. and Kaneko, J., "Combustion Chamber Shape and Pressurized Injection in High-Speed Direct-Injection Diesel Engines," SAE Trans. Vol.99, Paper No.900440, pp.960-974, 1990.
3. Minami, T., Yamaguchi, I., Shintani, M., Tsujimura, K. and Suzuki, T., "Analysis of Fuel Spray Characteristics and Combustion Phenomena under High Pressure Fuel Injection," SAE Tras. Vol.99, Paper No.900438, pp.948-959, 1990.
4. Suzuki, M., Nishida, K. and Hiroyasu, H., "Simultaneous Measurement of Fuel Vapor Concentration and Droplets Density in an Evaporating Diesel Spray with Laser Light Absorption and Scattering (1st Report, Development of Measuring Technique)," Transactions of the Japan Society of Mechanical Engineers, Vol.59, No.558, B, pp.329-337, 1993. (in Japanese)
5. Suzuki, M., Nishida, K. and Hiroyasu, H., "Simultaneous Concentration Measurement of Vapor and Liquid in an Evaporating Diesel Spray," SAE Paper, No.930863, pp.1-23, 1993.
6. Suzuki, M, Nishida, K. and Hiroyasu, H., "Imaging of Drop and Vapor Clouds in an Evaporating Fuel Spray by Ultraviolet and Visible Lasers," Proceedings of the 3rd International Congress on Optical Particle Sizing '93 - Yokohama, pp.363-370, 1993.